A MIMO Antenna with Enhanced Gain using Metasurface

Lan Ngoc Nguyen

Faculty of Electronics and Telecommunications, Saigon University, Vietnam
nnlan@moet.edu.vn

Abstract ─ This paper proposes a new metasurface to improve gain for dipole antenna. The antenna includes two sets of two elements (1 x 2), the integrated J shaped baluns, five metasurface cells (each metasurface cell consists of 5 periodic metallic plates printed on a thin low-cost FR4 substrate) for four antenna elements and the antenna is supplied by two T-junction power dividers. The metasurface is designed to operate as reflection surface. The antenna is designed based on RT5880 and witnesses an overall size of 140 x 37 x 35.075 mm^3 (2.7λ x 0.71λ x 0.67λ at 5.8 GHz), an isolation of approximately 28 dB, a peak gain of 9.5 dBi, and a radiation efficiency of 84%.

Index Terms ─ Dipole array, gain enhancement, metasurface, MIMO antenna.

I. INTRODUCTION

Metasurfaces are 2-D artificial material surfaces (MTSs) consisting of periodic arrangements of small inclusions in a dielectric host medium [1]. As its definition, MTSs are two-dimensional periodic structures and they are very thin compared to wavelength. Based on these features, MTSs can be divided into two categories, that are metafilm and metascreen. Recently, MTSs are a significant topic that are getting much attention of researchers thanks to highlight features such as less-lossy (due to having less physical space than 3D metamaterial structures), light-weight, easy fabrication, flexible [2]. Thanks to all above characteristics, there are wide ranges in applications of MTSs, for example: controllable smart surface [3], miniaturized cavity resonators [4], waveguide [5], biomedical devices [6] and so on [7], [8].

Besides, along with the development of modern wireless communication systems such as 5G, wireless local area network (WLAN), Global Positioning System (GPS), and so on, the demand for antennas with compact size, high gain and isolation, low cost has increased. A lot of antennas with different solutions to improve parameters have been reported, for example: artificial magnetic conductor (AMC) [9], defected ground structure (DGS) [10], epsilon negative transmission line (ENG-TL) [11], meander line [12]. In [9], the authors proposed an antenna for WLAN applications. Although the antenna achieves a high isolation (22 dB), gain is not good (7.3 dBi). Similarly, a magneto-electric dipole antenna with defected ground structure is presented in [10]. The antenna has a large bandwidth percentage (86.9%), but gain is only 7.2 dBi. This also appears with the proposed antennas in [11] and [12]. Moreover, antenna in [12] is a MIMO antenna, not only gain value is low (5.43 dBi), but also there is a low isolation (13 dB).

For the above reasons, a MIMO antenna dipole antenna with enhanced gain is presented in this paper. To enhance gain for antenna, metasurfaces are utilized and they are placed under each element. Here, metasurface acts as a reflective surface and its operating principle is based on Huygens–Fresnel principle. Each metasurface plate is a lattice including 5 metallic plates. In addition, to reduce cost, while the power dividers and elements are implemented on RT5880 (h = 1.575 mm, ε_r = 2.2, and tanδ = 0.0009), metasurfaces are realized on FR4 (h = 1.6 mm, ε_r = 4.4, and tanδ = 0.02). The antenna is designed for WLAN applications. At the 5.8 GHz, a peak gain value of 9.5 dBi and a high isolation of 28 dB are obtained. Furthermore, the antenna achieves a high efficiency of 84% at the resonant frequency. The measured results are compared to the simulated ones to verify the performance of the proposed antenna.

II. ANTENNA DESIGN

A. Metasurface structure

The unit-cell model of the metasurface structure is shown in Fig. 1 (a). The metallic plate is printed on the top side of FR4 substrate while the opposite side is ground plane. Initially, this model is constructed based on electric-LC resonator in [13]. By the modification in the shape of structure, the paper got a new structure as shown in Fig. 1 (a) while the reflection phase of the proposed structure is displayed in Fig. 1 (b). The configuration of metasurface includes a square at center and four squares at four corners.

The proposed structure yielded at the resonant frequency of 5.8 GHz. From Fig. 1 (b), we can see that the bandwidth of the proposed metasurface is 5.5 – 6.5 GHz for a fluctuation of reflection phase from -90° to +90° [14]. In which, the reflection phase is 0 degree at

Submitted On: December 27, 2020
Accepted On: February 23, 2021

https://doi.org/10.47037/2020.ACES.J.360412

5.9 GHz. It is clear that the proposed structure has a large bandwidth and it is enough to satisfy for operating range of frequency of antenna.

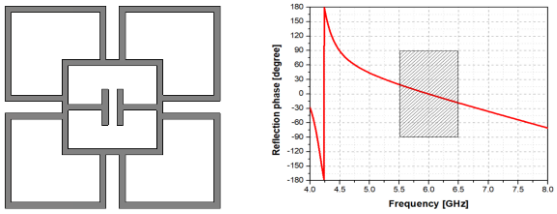

(a) (b)

Fig. 1. The metasurface structure: (a) the model of the unit-cell, and (b) reflection phase.

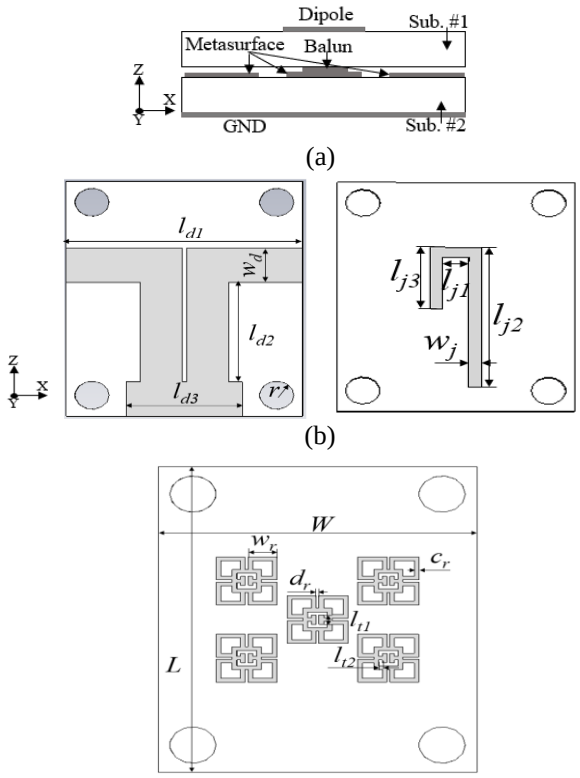

(a) (b) (c)

Fig. 2. The geometry of an antenna element: (a) cross-sectional view; (b) dipole and balun; (c) metasurface.

B. Geometry of the antenna

Firstly, Fig. 2 shows the geometry of an antenna element. It includes a dipole, a J shaped balun, a metasurface and ground plane. The dipole is printed on the upper side while J-shaped balun is placed on the bottom side of substrate-1. Similarly, there are metasurfaces at center of the top side and the opposite side is ground plane for substrate-2. Here, the kind of utilized dipole is half-wavelength at frequency of 5.8 GHz and it is realized on RT5880 (ε_r = 2.2, tanδ = 0.0009, and thickness of h = 1.575 mm). Meanwhile, metasurface is a lattice including 5 unit-cells, which is implemented on low-cost FR4 substrate (ε_r = 4.4, tanδ = 0.02, and thickness of h = 1.6 mm). In addition, four holes are created for using plastic piles to keep two substrates. Table 1 shows some parameters of an element.

In addition, an indispensable component in antenna array is power dividers. To achieve low profile and easy fabrication, T-junction power dividers is used and they are printed on RT5880 substrate. Fig. 3 (a) illustrates the model of power divider and its principle is presented in [15]. Because this is the equal power divider, in theory, S_{21} and S_{31} are -3dB. However, due to effect of mutual coupling and other reasons, S21 and S31 values are -3.3 dB at 5.8 GHz for simulation as shown in Fig. 3 (b). Table 2 shows some parameters of power divider. While the dimension of single antenna (1 x 2 elements) is 70 x 37 x 35.075 mm^3, the size of MIMO antenna is 140 x 37 x 35.075 mm^3 (MIMO antenna consists two set of two elements (1 x 2)).

Table1: Some parameters of an element

W	L	l_{d1}	w_d	l_{d2}	l_{d3}	r	l_{t1}
27.5	33.5	27.5	4.9	14.2	13.5	2	1
l_{j1}	l_{j2}	l_{j3}	w_j	w_r	c_r	d_r	l_{t2}
3	20.55	9	1.45	2.5	0.4	0.25	0.725

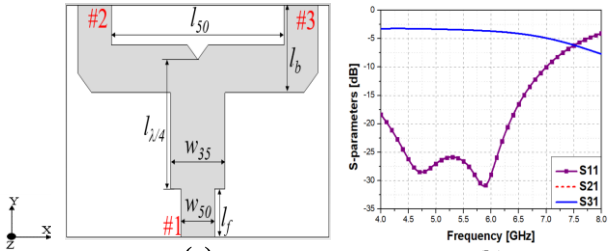

(a) (b)

Fig. 3. The model of power divider (a) and its S-parameters (b).

Table 2: Some parameters of power divider

l_{50}	l_b	w_{50}	l_f	$l_{\lambda/4}$	w_{35}
25	9.5	4.9	5.7	14.9	8

III. RESULTS AND DISCUSSION

As mentioned above, the goal of using metasurface in this paper is to enhance gain for antenna. In this case, metasurface acts as a reflection surface. For a better understanding, the paper simulates in two cases with and without metasurface and these simulated results are shown in Fig. 4.

Observe Fig. 4, we can see that the presence of metasurface is remarkably improved gain for antenna. To make it more specific, gain values are 8 dBi and 9.5

dBi at 5.8 GHz without and with metasurface, respectively. This gain enhancement is based on Huygens-Fresnel principle. We know that the Huygens-Fresnel principle said that each point on a primary wavefront can be considered to be a new source of a secondary spherical wave and it can be propagated according to a certain direction [16]. Therefore, in this case, when a plane wave comes on the metasurface, the total reflected energy flow from metasurface is the sum of reflection from all unit cells. If the phase of the total energy is same the phase of the excited wave in antenna, gain of antenna is enhanced. Switch to Fig. 4 (b), although the isolation of antennas is not improved at the frequency of 5.8 GHz, it is still better in the frequency range of 4.5 – 7.0 GHz (deeper). This shows that using metasurface not only enhances gain, but also improves isolation for antenna. To illustrate in more detail about gain enhancement for antenna, the paper demonstrates the difference in E- and H-fields between with and without metasurface. From Fig. 5, we can see that for the H-field, the maximum intensity value of antenna with metasurface (58.3 A/m) is greater than the one of antenna without metasurface (52.1 A/m). In contrast, for E-field, the maximum intensity value of antenna without metasurface is greater than the one with metasurface. This can be explained as follows. The radiation intensity is given by [16]:

$$U = \frac{1}{2} Re(E \times H^*) r^2, \quad (1)$$

with r is the distance.

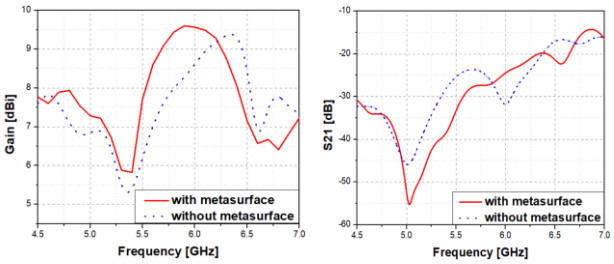

(a) (b)

Fig. 4. Gain values versus the frequency with and without metasurface.

In addition, the directivity is calculated:

$$D = \frac{U}{U_0}, \quad (2)$$

with U_0 is radiation intensity of isotropic source.

Then, gain of antenna can be expressed as:

$$G = eD = \frac{e\left[\frac{1}{2} Re(E \times H^*) r^2\right]}{U_0}, \quad (3)$$

in which e is the radiation efficiency of antenna. Therefore, although the maximum intensity value of antenna with metasurface is smaller than the one of antenna without metasurface in E-field, gain of antenna with metasurface is better than without metasurface. This is because the radiation intensity of antenna (H-field) with metasurface (U) is much greater than the one of antenna without metasurface. As a result, the product of E- and H-field with metasurface is still greater than the one of E- and H-filed without metasurface.

Figure 6 illustrates simulated gain for the different lengths of metasurface substrate (L in Table 1) and the various sizes of unit cell (w_r in Table 1).

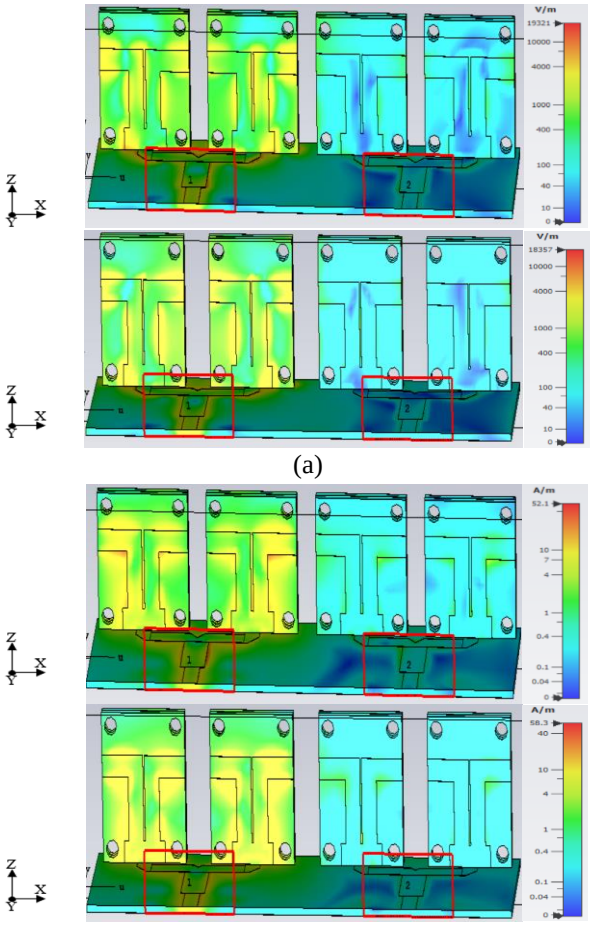

(a) (b)

Fig. 5. The intensity of E-field (a) and H-field (b): without metasurface (up) and with metasurface (down) when the first element is excited.

From Fig. 6 (a), we can see that at the frequency of 5.8 GHz, gain of antenna increases with increasing the length of metasurface (L) substrate while the isolation is guaranteed under -25 dB in three cases. Meanwhile, the isolation of antenna is improved better (compared to the change of the metasurface length (L)) with the different sizes of unit cell (w_r) (Fig. 6 (b)). In contrast, gain of antenna with the various lengths of substrate is better than the one of various dimensions of unit cell. For the reflection coefficient, there is no significant difference and the resonant frequency is ensured in all above cases. This shows that while the changes of w_r improve the

isolation, the changes of L enhance gain for antenna. By combining the changes of both above parameters, the paper achieves an improvement for both gain and isolation. Finally, the optimized dimensions of L and w_r are 33.5 and 2.5 mm, respectively.

To verify the performance of the proposed antenna, the prototypes of MIMO antenna are fabricated and shown in Fig. 7. The size of an element is 33.5 x 27.5 x 3.175 mm^3 while the dimensions of single antenna and MIMO antenna are 70 x 37 x 35.075 mm^3 and 140 x 37 x 35.075 mm^3, respectively. Moreover, the elements including dipole antennas, baluns, power dividers are based on RT5880 (h = 1.575 mm, ε_r = 2.2, and tanδ = 0.0009) while metasurface is implemented on FR4 (h = 1.6 mm, ε_r = 2.2, and tanδ = 0.0009). The measurement of antenna is implemented at Laboratory of Monolithic Microwave Integrated Circuit (MMIC) & Applications for Embedded Systems – International University, VNU HoChiMinh City, Vietnam. The computed and measured results consisting of the reflection coefficient, pattern and directivity of the proposed antenna are compared together and shown in Fig. 8 and Fig. 9. Observe Fig. 8, we can see that there is a better impedance matching in simulated result at resonant frequency. However, the measured and simulated results are quite similar. In addition, the working frequency range (from 5.74 GHz to 5.99 GHz) is still ensured under -10 dB and the mutual coupling is -28 dB (for both simulation and measurement).

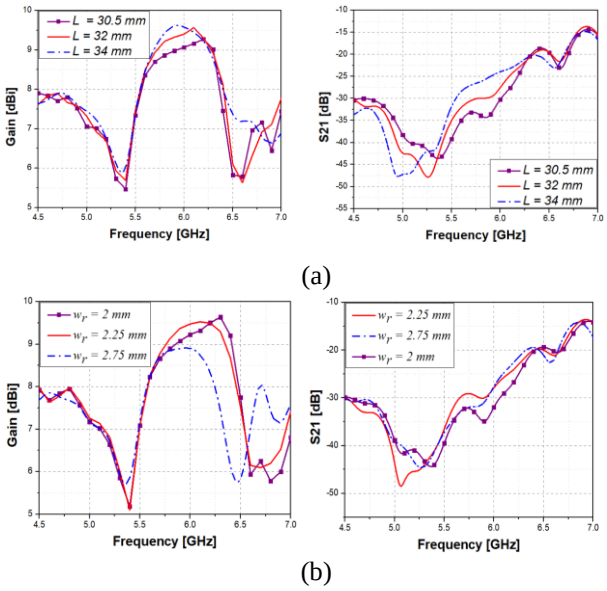

Fig. 6. Simulated gain versus the different lengths of metasurface substrate (a), and various sizes of unit cell (b).

Switch to Fig. 9, we can see that there is a difference between simulated and measured results in xz and yz planes. Here, the directivity of the MIMO antenna for simulation is 10.16 dBi while this value for measurement is 8.8 dBi at 5.8 GHz. This tolerance can be caused from attenuation of FR4. However, the shapes of planes are quite similar. In addition, as mentioned above, using metasurface enhances gain for antenna by combining all reflection flows from all unit cells that they are the same phase. Then, the phase of the total flow from reflection can be shifted compared to normal case (0^o). As a result, there is a slight shift in the main lobe of antenna as in Fig. 9. In addition, there is a difference between simulation and measurement results in xz and yz planes of antenna. This error can be contributed from mistakes in the fabrication progress. Moreover, the test environment is not ideal and this leads the tolerance in antenna measurement. However, these results are acceptable. Moreover, the efficiency of antenna achieves over 84%.

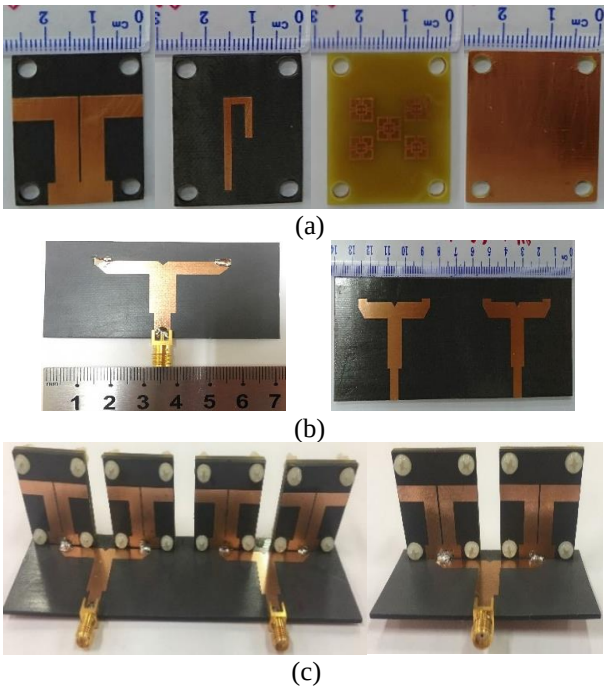

Fig. 7. The prototypes of the proposed antenna: (a) dipole, balun, metasurface and ground; (b) power dividers; (c) single array and MIMO antenna.

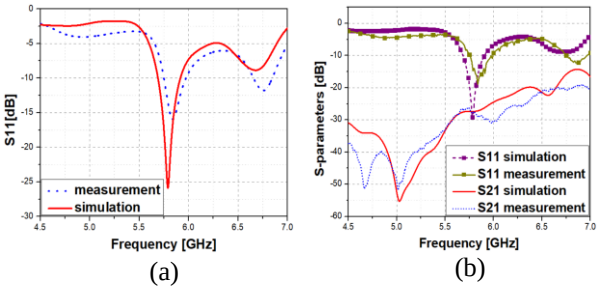

Fig. 8. The measurement results of the reflection coefficient: (a) single array; (b) MIMO antenna.

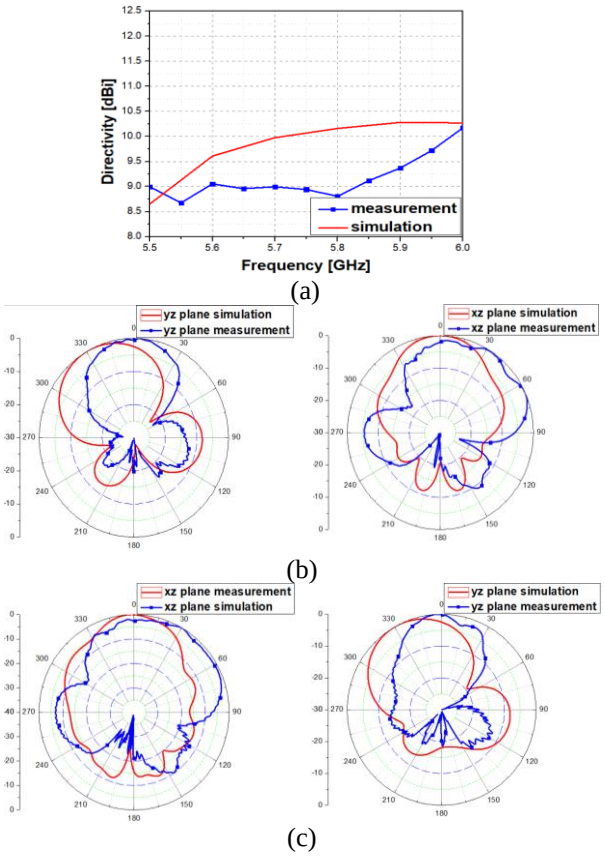

Fig. 9. The measured results of pattern and directivity of the proposed antenna: (a) directivity, (b) xz and yz planes of single array; (c) xz and yz planes of MIMO antenna.

Figure 10 illustrates the enveloped correlation coefficient (ECC) of the MIMO antenna. Here, ECC is calculated by using formula in [17]:

$$\rho_e = \frac{|S_{11}^* S_{12} + S_{21}^* S_{22}|^2}{(1-|S_{11}|^2-|S_{21}|^2)(1-|S_{22}|^2-|S_{12}|^2)}. \quad (4)$$

It is clear that the ECC of the proposed antenna is less than 0.0025 in a wide frequency range from 5 GHz to 6 GHz. This shows that the proposed antenna is enough to respond for MIMO applications.

Table 3 shows a performance comparison among the proposed antenna and recent MIMO antennas. It should be noted that the proposed antenna concentrates gain enhancement. In addition, it is difficult to find MIMO arrays in papers. Currently, MIMO antennas in papers are mostly MIMO single antenna (it means that MIMO antenna has n ports in which each port is an element) while the proposed antenna is two elements in each port. As a result, the size of the proposed antenna is larger and this is natural. Observing Table 3, we can see that antenna in [18] has a large bandwidth percentage (29.6%) and a high efficiency (85%); however, the isolation between elements is low (15dB). Similarly, an dual band and dual polarization log-periodic dipole array is proposed for MIMO WLAN applications [19]. Although this antenna achieves a wide impedance bandwidth (10% and 24%) and a low mutual coupling (-20 dB), gain of antenna is only 6 dBi. In addition, this MIMO antenna includes 12 elements (6 elements for horizontal polarization and 6 elements for vertical polarization) and a high complexity. Meanwhile, there is a narrow bandwidth of the proposed antennas in [19] and [20] although the isolations are high (20 and 40 dB). Moreover, gain of the antenna in [21] is not good (4 dB).

Table 3: The comparison among the proposed antenna and recent MIMO antennas

References	[18]	[20]	[21]	[19]	[22]	**My work**
Frequency [GHz]	2.6	2.45	2.4	2.4/5.5	2.55	5.8
Bandwidth [%]	29.6	2.5	2.2	10/24	56	4.3
Isolation [dB]	15	20	40	20	10	28
Efficiency [%]	85	x	x	x	<90	84
Gain [dBi]	x	x	4	6	4	9.5
Size (λ)	0.69 x 0.69 x 0.014	0.82 x 0.65 x 0.013	0.96 x 0.96 x 0.18	1.2 x 1.2 x 0.48	0.85 x 0.85 x 0.21	2.7 x 0.71 x 0.67

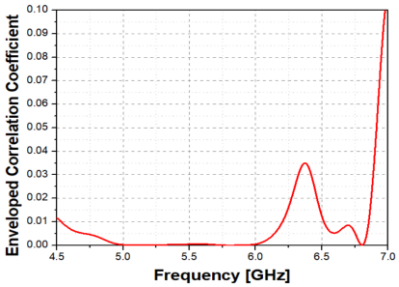

Fig. 10. The enveloped correlation coefficient of the proposed MIMO antenna.

IV. CONCLUSION

A MIMO dipole antenna with enhanced gain by using metasurface is proposed in this paper. The antenna array consists of two sets of two elements (1 x 2) dipole antenna with an overall dimension of 140 x 37 x 35.075 mm^3. While the elements, baluns and power dividers are fabricated on RT5880 substrate, metasurface is printed on FR4 substrate. The antenna is yielded at 5.8 GHz and witnesses a measured $|S_{11}|$ < -10 dB bandwidth of 5.74-5.99 GHz (4.3%). In addition, the proposed antenna resulted in a pick gain 9.5 dBi (at 5.8 GHz), a radiation efficiency of 84% and a high isolation of approximately 30 dB. With the above achieved results along with

advantages such as low profile and, low cost and easy fabrication, the proposed antenna is a good candidate for utilizing in wireless communication systems.

ACKNOWLEDGEMENT

This paper is carried out in the framework of the project titled Design of dipole antenna with high gain using reflective surface under the Grant number TĐ2020-18. The author would like to thank the Saigon University, Vietnam for their financial support.

REFERENCES

[1] M. Faenzi, G. Minatti, D. González-Ovejero, F. Caminita, E. Martini, C. Della Giovampaola, and S. Maci, "Metasurface antennas: New models, applications and realizations," *Scientific Reports*, vol. 9, no. 1, pp. 1-14, 2019.

[2] C. L. Holloway, E. F. Kuester, J. A. Gordon, J. O'Hara, J. Booth, and D. R. Smith, "An overview of the theory and applications of metasurfaces: The two-dimensional equivalents of metamaterials," *IEEE Antennas and Propagation Magazine*, vol. 54, no. 2, pp. 10-35, 2012.

[3] Q. Ma, G. D. Bai, H. B. Jing, C. Yang, L. Li, and T. J. Cui, "Smart metasurface with self-adaptively reprogrammable functions," *Light: Science and Applications*, vol. 8, no. 1, pp. 1-12, 2019.

[4] M. Caiazzo, S. Maci, and N. Engheta, "A metamaterial surface for compact cavity resonators," *IEEE Antennas and Wireless Propagation Letters*, vol. 3, no. 1, pp. 261-264, 2004.

[5] Z. Li, M.-H. Kim, C. Wang, Z. Han, S. Shrestha, A. C. Overvig, M. Lu, A. Stein, A. M. Agarwal, M. Lončar, and N. Yu, "Controlling propagation and coupling of waveguide modes using phase-gradient metasurfaces," *Nature Nanotechnology*, vol. 12, no. 7, pp. 675-683, 2017.

[6] L. La Spada, "Metasurfaces for advanced sensing and diagnostics," *MDPI-Sensors (Switzerland)*, vol. 19, no. 2, p. 355, 2019.

[7] J. Guo, T. Wang, H. Zhao, X. Wang, S. Feng, P. Han, W. Sun, J. Ye, G. Situ, H.-T. Chen, and Y. Zhang, "Reconfigurable terahertz metasurface pure phase holograms," *Advanced Optical Materials*, vol. 7, no. 10, pp. 1-7, 2019.

[8] J. A. Gordon, C. L. Holloway, J. Booth, S. Kim, Y. Wang, J. Baker-Jarvis, and D. R. Novotny, "Fluid interactions with metafilms/metasurfaces for tuning, sensing, and microwave-assisted chemical processes," *Physical Review B - Condensed Matter and Materials Physics*, vol. 83, no. 20, pp. 1-5, 2011.

[9] H. Zhai, K. Zhang, S. Yang, and D. Feng, "A low-profile dual-band dual-polarized antenna with an AMC surface for WLAN applications," *IEEE Antennas and Wireless Propagation Letters*, vol. 16, no. 61501341, pp. 2692-2695, 2017.

[10] J. Zeng and K. M. Luk, "A simple wideband magnetoelectric dipole antenna with a defected ground structure," *IEEE Antennas and Wireless Propagation Letters*, vol. 17, no. 8, pp. 1497-1500, 2018.

[11] E. Kantola, J. Penttinen, S. Ranta, and M. Guina, "Metamaterial based circularly polarized antenna employing ENG-TL with enhanced bandwidth for WLAN applications," *Electronics Letters*, vol. 54, no. 20, pp. 1152-1154, 2018.

[12] S. Chouhan, D. K. Panda, M. Gupta, and S. Singhal, "Meander line MIMO antenna for 5.8 GHz WLAN application," *International Journal of RF and Microwave Computer-Aided Engineering*, vol. 28, no. 4, e21222, 2018.

[13] W. Withayachumnankul, C. Fumeaux, and D. Abbott, "Compact electric-LC resonators for metamaterials," *Optics Express*, vol. 18, no. 25, pp. 25912-25921, 2010.

[14] T. N. Hien Doan, S. X. Ta, K. Van Nguyen, K. K. Nguyen, and C. Dao-Ngoc, "Low-profile, dual-band, unidirectional RFID tag antenna using metasurface," *Progress In Electromagnetics Research C*, vol. 93, no. May, pp. 131-141, 2019.

[15] D. M. Pozar, *Microwave Engineering*. Third ed., John Wiley & Sons, Inc., 2005.

[16] C. A. Balanis, *Antenna Theory: Analysis and Design*, Third Ed., John Wiley & Sons, 2005.

[17] S. Blanch, J. Romeu, and I. Corbella, "Exact representation of antenna system diversity performance from input parameter description," *Electronics Letters*, vol. 39, no. 9, pp. 705-707, 2003.

[18] Y. Zhang and P. Wang, "Single ring two-port MIMO antenna for LTE applications," *Electronics Letters*, vol. 52, no. 12, pp. 998-1000, 2016.

[19] J. J. Liang, J. S. Hong, J. B. Zhao, and W. Wu, "Dual-band dual-polarized compact log-periodic dipole array for MIMO WLAN applications," *IEEE Antennas and Wireless Propagation Letters*, vol. 14, no. c, pp. 751-754, 2015.

[20] H. Arun, A. K. Sarma, M. Kanagasabai, S. Velan, C. Raviteja, and M. G. N. Alsath, "Deployment of modified serpentine structure for mutual coupling reduction in MIMO antennas," *IEEE Antennas and Wireless Propagation Letters*, vol. 13, pp. 277-280, 2014.

[21] G. Zhai, Z. N. Chen, and X. Qing, "Enhanced isolation of a closely spaced four-element MIMO antenna system using metamaterial mushroom," *IEEE Transactions on Antennas and Propagation*, vol. 63, no. 8, pp. 3362-3370, 2015.

[22] E. Fritz-Andrade, R. Gómez-Villanueva, J. A. Tirado-Méndez, L. A. Vasquez-Toledo, A. Rangel-Merino, and H. Jardón-Aguilar, "Broadband four elements pifa array for access-point mimo systems,"

Progress in Electromagnetics Research C, vol. 106, pp. 163-176, 2020.

Lan Ngoc Nguyen received Ph.D. degree from School of Electronics and Telecommunications, Hanoi University of Science and Technology in 2019. Currently, she is a Lecturer at Faculty of Electronics and Telecommunications, Saigon University, Vietnam. Her research interests are microstrip antenna, mutual coupling, MIMO antennas, array antennas, reconfigurable antennas, polarization antennas, metamaterial, metasurface. ORCID: https://orcid.org/0000-0001-8506-9979